28-GHz Indoor Channel Measurements and Analysis of Propagation Characteristics

Mingyang Lei, Jianhua Zhang, Tian Lei, Detao Du
Key Laboratory of Universal Wireless Communications,
Wireless Technology Innovation Institute, Ministry of Education, China
Beijing University of Posts and Telecommunications, Beijing, 100876, China
Email: andyray1990@163.com

***Abstract*—In this paper, we present an indoor channel measurement system at 28 GHz and analysis result of propagation characteristics. The measurement system consists of a vector network analyzer (VNA) and a pair of 26 dBi horn antennas. It makes reliable wireless links with a maximum distance up to 30 meters. Measurement campaign was conducted in Beijing with three different indoor scenarios including office, corridor and hall. Power delay profiles (PDPs) are derived from raw data measured in four transmitter locations and 101 receiver locations. On this basis, three types of propagation characteristics including path loss, root mean square (RMS) delay spread and power angular profiles (PAPs) are analyzed. The results show that indoor environments can enhance received signal power in LOS case. However, in NLOS condition penetration loss caused by wall and door may bring considerable attenuation, which implies that smaller cells will play an important role on increasing the probabilities of LOS links for the future communication systems. Multipath components (MPCs) can be detected in several directions although using high-directional antennas.**

I. Introduction

In the past decade, mobile networks have experienced an explosive growth and lead to a boom in new data services and applications. The rapid increasing wireless data traffic expects huge bandwidth in future communication systems. Millimeter wave characterizes electromagnetic wave whose frequency lies between 26.5 and 300 GHz. Millimeter wave communication system is a fast emerging technology with uniquely attractive features of unprecedented broad bandwidth. With no doubt it will satisfy the demand of high data rate for future mobile network users.

Capacity of the wireless communication system is determined by the propagation characteristics of the radio channel. Therefore, it is necessary to investigate the propagation characteristics of millimeter wave through channel measurement and provide fundamental theoretical basis for the design, evaluation and actual deployment for future mobile networks [1].

There have been studies about millimeter wave channel measurement. Propagation characteristics at 28 GHz have been reported in [2,3], which mainly concentrate on the outdoor scenarios. Reflection coefficients and penetration losses for common building materials at 28 GHz have been presented in [4]. Research in [5,6] mainly concerns the propagation characteristics at e-bands. However, the bandwidth of baseband signal is strongly restricted by hardware performance and higher frequency will lead to considerable cost. Thus, frequency spectrum around 28 GHz will be a relatively optimized choice to support the bandwidth in future communication systems. Moreover, millimeter wave communication system will be mainly used in hot spots, especially for indoor scenarios instead of long-range coverage. Few literatures paid their attention on the propagation characteristics of indoor scenarios at 28 GHz.

In this paper, we lay emphasis on investigating the propagation characteristics of indoor radio channel based on our channel measurement at 28 GHz. The channel frequency response is accurately captured and channel impulse response (CIR) is obtained via IFFT. Path loss, RMS delay spread and PAP in three different scenarios will be analyzed and compared. These empirical results could provide a reference for the design of future communication systems.

The remainder of this paper is organized as follows. The measurement system and experimental method are explained in Section II. Data processing and parameter estimation are described in Section III. Results and analysis of propagation parameters are discussed in Section IV. Section V summarizes the results of this work and concludes this paper.

II. Measurement Description

A. Measurement Setup

Measurements were conducted in frequency-domain where the channel frequency response, $H(f)$, was measured and stored. The measurement system consists of a VNA, a 56 dB gain wideband power amplifier, a 50 dB gain low-noise amplifier and a pair of wideband horn antennas with 3 dB beamwidth of 10°, as is shown in Fig. 1. The VNA was remotely controlled by labVIEW software so that data could be captured automatically. The measured data was temporarily stored in VNA and then transferred to a laptop hard drive via an Ethernet interface. A 30 m-link in this measurement system could achieve a signal-to-noise ratio (SNR) of 16.6 dB, which satisfies the threshold of general modulation types [7]. The calculation method is described in [8].

In our measurement campaign, the center frequency of VNA was set to 28 GHz. A total of 200 samples were uniformly distributed on the 1 GHz frequency bandwidth, which led to a frequency step of 5 MHz. Thus, the maximum

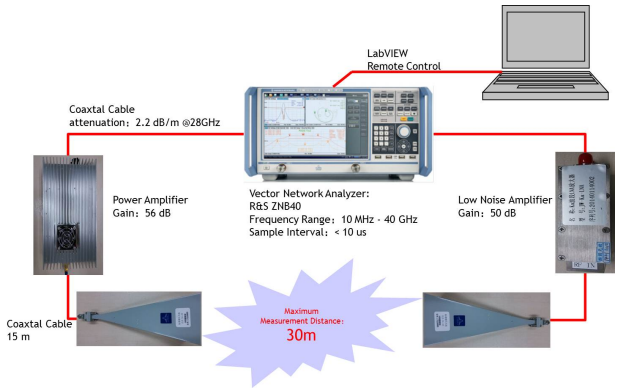

Fig. 1. Measurement system.

measurable excess delay was determined to be 200 ns, and the corresponding maximum measurable distance was 60 m. Each of the frequency points was sampled 200 times in time-domain, and we calculated an average to offset the small-scale fading caused by time-variant channel. According to [9], measuring time for each sample point was less than 10 us, which meant in each spatial point the total measuring time for integrated measurement with 200 samples both in the frequency and time-domain was less than 0.4 s. In this procedure, no pedestrians appeared in the scenarios and we assumed that the channel kept quasi-static. Finally, The VNA measured the $H(f)$ of 28 GHz channel. Parameters of our measurement system are summarized in table I.

TABLE I
MEASUREMENT SYSTEM PARAMETERS

Parameter	value
Center frequency	28 GHz
Bandwidth	1 GHz
Sweep count (frequency-domain)	200
Sweep count (time-domain)	200
Frequency step	5 MHz
TX power	30.6 dBm
Scenario	Indoor
TX antenna number	1
RX antenna number	1

B. Measurement Environment

We conducted our measurement in the 1st and 7th floor of the New Building of Technology and Research (NBTR) at Beijing University of Posts and Telecommunications. The actual measurement environments are shown in Fig. 2. The corresponding layouts are illustrated in Fig. 3, 4 and 5. A total of 4 TXs and 101 RXs were set in these environments. Among them each combination of the TX antenna and RX antenna were adjusted towards each other to make a LOS link. Antennas were mounted on a tripod and were able to be moved freely to any directions. All the height of the TX antennas were set to 1.93 m while the height of the RX antennas were set to 1.75 m. The purpose of these settings is listed as follows.

Measurements in TX1-TX3 were aimed at calculating the path losses and RMS delay spreads in three indoor scenarios of different size. TX1 was in the hall located in the 1st floor of NBTR. It was identified as a relatively large scenario. TX2 was situated in office room 717 whose propagation environment was of medium-size. The narrow corridor out of room 717 was chosen to be the minimum-size scenario. TX4 was set out of room 729 to measure PAP of a specific receiver site, as is shown in Fig. 11. The surrounding walls, floor, ceiling and furniture generated abundant MPCs. We fixed RX at a typical position and rotated the receiver antenna in azimuth from 0° to 360° with a step size of 10° and $H(f)$ were captured at each of the 36 angular steps.

Fig. 2. Scenarios of the measurements. The one in top-left corner was captured in the hall of NBTR. On its right side, the scen of office room 717 in NBTR is shown. The one in bottom-left corner is the view of corridor outside room 717. The last image presents the scenario of PAP measurement.

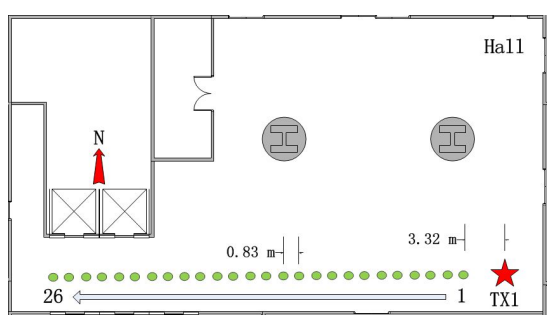

Fig. 3. Lay out of the hall in NBTR. Each green dot represents a specific RX site. Distance between two adjacent RXs is 0.83 m. Measurement route is indicated by the line with an arrow.

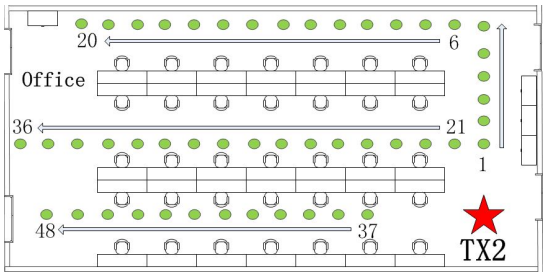

Fig. 4. Lay out of office room 717 in NBTR. The length, width and height are 11.4 m, 7.8m and 3m, respectively. The maximum height of office furniture is about 1 m. Distance between two adjacent RXs is 0.6 m. Walls around the office are made of bricks.

Fig. 5. Lay out of corridor outside room 717 in NBTR. The height of corridor is 2.5 m while the width is 2.2 m. Distance between two adjacent RXs is 0.6 m. Floors are paved with smooth tiles in all scenarios.

III. Measurement Data Processing and Estimation of Propagation Parameters

A. Data Processing Method

After the measurement procedure, raw data acquired from VNA is the discrete samples of channel response, $H(f)$, in frequency-domain. There are 3 steps of data processing, i.e., data window adding, IFFT and noise cutting, which are essential to close the real channel information [10]. Loss of signal power is less than 5% when all these steps are completed. We define the CIR for a single sample in time-domain as $h_{i,s}(\tau)$. We calculate the average of all the samples to avoid the fading probably existing in our measurement as follows

$$\bar{h}_s(\tau) = \frac{1}{N_T}\sum_{i=1}^{N_T} h_{i,s}(\tau), s = 1, ..., N_S \tag{1}$$

where N_T and N_S are the number of samples in time-domain and spatial-domain, respectively; i represents the index of sample in time-domain, s refers to the specific measured point in spatial-domain.

B. Path loss

Power delay profile (PDP) reveals the power strength of received signal and travel time of arrived resolvable multi-paths. Based on the data processing, PDP is defined as

$$p_s(\tau) = \left|\bar{h}_s(\tau)\right|^2. \tag{2}$$

Path loss characterizes the reduction in power density from the transmitter to the receiver and is defined by the ratio of transmitted power to received power. Cable losses, amplifier gains and insertion losses brought by connectors between the system components are all calibrated. Path loss is calculated as

$$PL_s = -10\log_{10}\left(\sum_{l=1}^{T} p_s(\tau_l)\right) + G_{TX} + G_{RX} \tag{3}$$

where T is the length of $h_i(\tau)$ and $P_s(\tau)$, the later two algebraic terms in sequence are TX and RX antenna gains in dBi.

On the measured frequency band, the maximum and minimum gain of antennas are 27.1 dBi and 26.1 dBi, respectively. Thus, the gain fluctuation is about 1 dBi. This value is 3 dB for amplifier. Considering the potential errors caused by these fluctuations, path loss in free space is utilized to perform a calibration

$$PL'_s = PL_s - PL_s(d_0) + PL_{freespace}(d_0) \tag{4}$$

where d_0 equals to 5 meters. The difference between PL'_s and PL_s is defined as excess loss [11].

C. RMS delay spread

This parameter indicates the propagation quality of multipath channel. Delay spread characterizes the difference between the maximum excess delay and the minimum one. RMS delay spread can be calculated by the second central moment of power delay profile, which is obtained by

$$\tau_{rms} = \sqrt{\frac{\sum_s \tau^2 \cdot P_s(\tau)}{\sum_s P_s(\tau)} - \left(\frac{\sum_s \tau \cdot P_s(\tau)}{\sum_s P_s(\tau)}\right)^2}. \tag{5}$$

D. Power angular profile (PAP)

PAP shows the power intensity of received signal in 360° azimuth. PDP was integrated to power

$$P_k = \int_{-\infty}^{\infty} p_k(\tau)d\tau, k = 1, ..., 36 \tag{6}$$

where $p_k(\tau)$ is the PDP calculated in each azimuth direction and its corresponding power is represented by P_k. Then the following operation was done

$$r_k = 10\log_{10}\frac{P_k}{\min\{P_1, ..., P_{36}\}} \tag{7}$$

r_k is shown in a polar plot which indicates the relative power intensity of received signal in various directions.

IV. Measurement Result and Analysis

Based on the parameter estimation method described above, propagation characteristics including PDP, path loss, RMS delay spread and PAP are analyzed in this section.

A. PDP

Fig. 6 presents a PDP result at RX point 2 in the office scenario. While the τ axis represents the CIR information in delay-domain and the t axis identifies the time-varying characteristics. It is obvious that the channel is quasi-static in the measurement of a single spatial point. More than three paths are observed and the strongest one is brought by LOS propagation whose power intensity is about -10 dB. Others are

caused by reflectors (floor, ceiling, walls, etc.), among which the strongest power is 20 dB lower than LOS path. The noise level is about -70 dB and leads to a large dynamic range of 60 dB. Although the τ axis characterizes CIR in delay-domain, it is important to notice that the delay value is not absolutely accurate due to the extra delay brought by cable and converters in measurement system. But the relative delay between paths can be accurately captured.

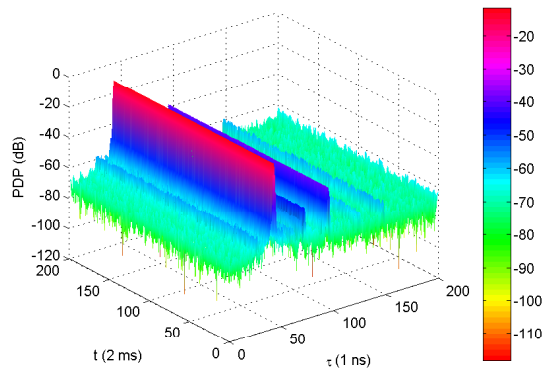

Fig. 6. PDP result at RX point 2 in the office scenario.

B. Path loss

Path losses in three scenarios are illustrated in Fig. 7. The red, blue and green curves fit measured path losses with the minimum mean square error rule. Path loss in free space is also presented for visual comparison. It is worth noting that the path loss exponents (PLEs) have a strong correlation with propagation environments. The open field in hall scenario is similar to free space and its PLE is 2.2. Office is of smaller size compared with hall and its PLE reduces to 1.8 resulted from the surrounding reflectors. In corridor, PLE even decreases to 1.2 because of the wave guide effect caused by the narrow passage. Therefore, in indoor LOS conditions, PLEs fluctuate about 2, while in NLOS outdoor case PLEs increase to 5.76 [2]. A positive correlation between excess loss and TX-RX separation is found. In our measurement, excess losses varies from 5 dB to 10 dB.

C. RMS delay spread

The RMS delay spread is extracted as it is illustrated in Section III. Fig. 8, 9 and 10 present the distributions of RMS delay spread in office, corridor and hall scenarios, respectively. It can be found that RMS delay spread is closely related to its corresponding propagation environment. In office the mean value of RMS delay spread is 42.8 ns and in corridor it grows to 56.037 ns. This difference can be explained by the longer distance between TX and RX in the later scenario. Its narrow propagation environment also contributes a lot of MPCs for the received signal. In hall, this value is 57.9 ns, slightly larger than the one in corridor. Besides, all the measured RMSs can be fitted well by normal distribution.

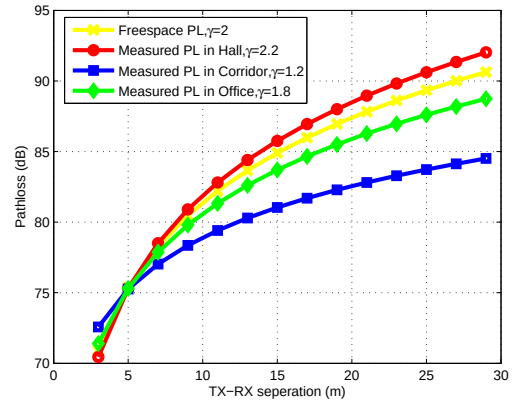

Fig. 7. Calibrated path loss, γ represents PLE.

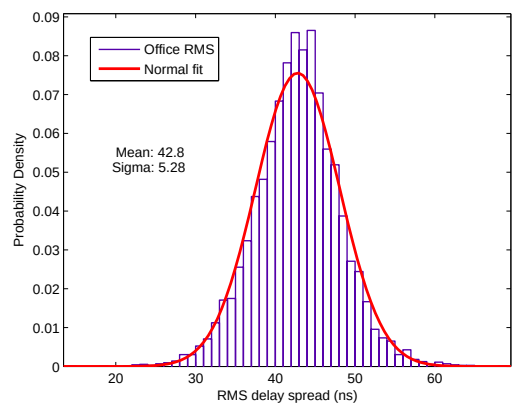

Fig. 8. PDF of RMS delay spread in office.

D. PAP

PAP is investigated in this section. The PAP result shown in Fig. 11 is generated by two steps. First, each r_k of 36 combinations distinguished by directions of RX antennas are calculated and presented in the polar plot. Second, we import the diagram into the specific site-map according to actual scale. It is observed that the power of LOS path is 30 dB higher than the lowest one among all the directions. Another MPC whose power intensity is 10 dB lower than LOS path and reflected by the glass wall is detected. There are also several remaining detected paths whose power intensities are lower than 10 dB. These MPCs may arrive at the receiver through more than one bounces. This result implies the possibility of modeling channels with the ray tracing method in indoor scenarios [12].

V. Conclusion

In this paper, a measurement system mainly consisting of a VNA and a pair of horn antennas for indoor channel measurements at 28 GHz is presented. The maximum measurement range is 30 meters which is sufficient for common indoor measurements. The measurement campaign was performed in

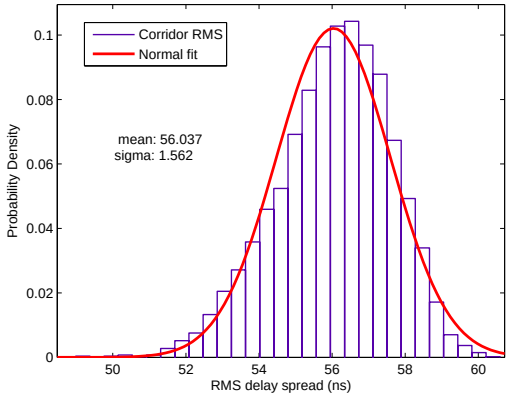

Fig. 9. PDF of RMS delay spread in corridor.

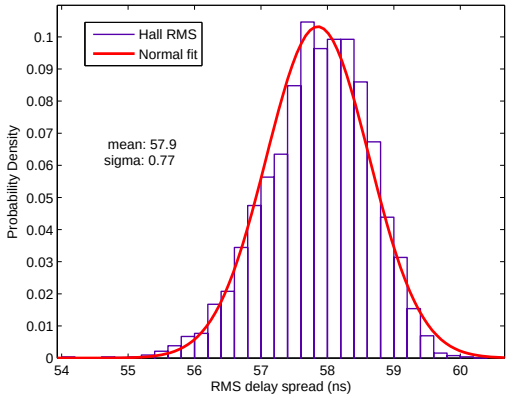

Fig. 10. PDF of RMS delay spread in hall.

three different scenarios: office, corridor and hall. On this basis, propagation characteristics including PDP, path loss, RMS delay spread and PAP were measured. Analysis results show strong correlations between propagation characteristics and the radio channel environments. PLEs in hall, office and corridor are 2.2, 1.8 and 1.2 in sequence and excess loss ranges from 5 dB to 10 dB. RMS delay spread is about 50 ns in indoor scenarios and has positive correlation with the size of propagation environments. Though LOS path play the dominant role, abundant MPCs were generated during propagation. Received signal can be detected in different directions. The method of receiving these signals effectively with directional antennas is highly significant in further studies. Generally the spatial size of indoor scenarios are relatively small. Thus, ray tracing method of channel modeling becomes feasible.

Acknowledgment

The research is supported by National Natural Science Foundation of China (NO. 61322110), National Science and Technology Major Project of the Ministry of Science and Technology (2013ZX03003009-002), Program for New Century Excellent Talents in University of Ministry of Education of China (NCET-11-0598), National 863 Project of the Ministry of Science and Technology (2014AA01A706), the Ph.D. Programs Foundation of Ministry of Education of China (NO. 20130005110001).

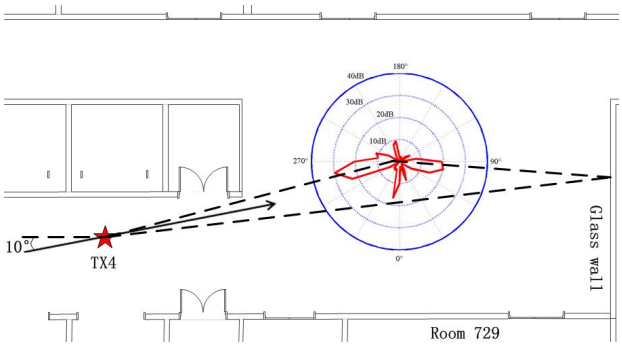

Fig. 11. PAP of the received signal. The black arrow represents the direction of TX antenna.

References

[1] J. Zhang, "Review of wideband MIMO channel measurement and modeling for IMT-Advanced systems," *Chinese Science Bulletin*, vol. 57, no. 19, pp. 2387-2400, 2012.

[2] Y. Azar, G. N. Wong, K. Wang, R. Mayzus, J. K. Schulz, H. Zhao, F. Gutierrez, D. Hwang, and T. S. Rappaport, "28 GHz propagation measurements for outdoor cellular communications using steerable beam antennas in New York City," *2013 IEEE International Conference on Communications (ICC)*, pp. 5143-5147.

[3] M. Samimi, K. Wang, Y. Azar, G. N. Wong, R. Mayzus, H. Zhao, J. K. Schulz, S. Sun, F. Gutierrez, and T. S. Rappaport, "28 GHz angle of arrival and angle of departure analysis for outdoor cellular communications using steerable beam antennas in New York City," *2013 IEEE 77th Vehicular Technology Conference (VTC Spring),* pp. 1-6.

[4] H. Zhao, R. Mayzus, S. Sun, M. Samimi, J. K. Schulz, Y. Azar, K. Wang, G. N. Wong, F. Gutierrez, and T. S. Rappaport, "28 GHz millimeter wave cellular communication measurements for reflection and penetration loss in and around buildings in New York City," *2013 IEEE International Conference on Communications (ICC),* pp. 5163-5167.

[5] H. Zhang and U. Madhow, "Statistical modeling of fading and diversity for outdoor 60 GHz channels," *Proceedings of the 2010 ACM international workshop on mmWave communications: from circuits to networks,* pp. 45-50.

[6] S. Nie, G. R. MacCartney, S. Sun, and T. S. Rappaport, "72 GHz millimeter wave indoor measurements for wireless and backhaul communications," *2013 IEEE 24th International Symposium on Personal Indoor and Mobile Radio Communications (PIMRC),* pp. 2429-2433.

[7] A. F. Molisch, *Wireless communications*. John Wiley & Sons, 2010, vol. 15.

[8] H. Yang, P. F. Smulders, and M. H. Herben, "Channel characteristics and transmission performance for various channel configurations at 60 GHz," *EURASIP Journal on Wireless Communications and Networking*, vol. 2007, no. 1, pp. 43-43.

[9] "R&S, ZNB Vector Network Analyzer Specifications," August 2013. [Online]. Available: http://cdn.rohde-schwarz.com/dl_downloads/dl_ common_library/dl_brochures_and_datasheets/pdf_1/ZNB_dat-sw_ en_5214-5384-22_v0700.pdf

[10] C. Lian, "Indoor wireless channel measurement and analysis at 6.25 GHz based on labview," *2011 10th International Conference on Electronic Measurement & Instruments (ICEMI),* vol. 1, pp. 252-257.

[11] P. Soma, L. C. Ong, S. Sun, and M. Y. Chia, "Propagation measurements and modeling of LMDS radio channel in Singapore," *IEEE Transactions on Vehicular Technology,* vol. 52, no. 3, pp. 595-606, 2003.

[12] H. Xu, V. Kukshya, and T. S. Rappaport, "Spatial and temporal characteristics of 60-GHz indoor channels," *IEEE Journal on Selected Areas in Communications,* vol. 20, no. 3, pp. 620-630, 2002.